A graphical Abstract

Inspired by the bio-adhesive ability of the marine mussel, highly hydrogen permselective ZIF-8 membranes with “reinforced concrete” structure were prepared on polydopamine functionalized macroporous inexpensive stainless-steel-nets.

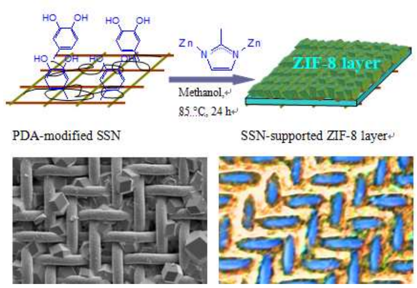

Cite this: DOI: 10.1039/c0xx00000x

www.rsc.org/xxxxxx

ARTICLE TYPE

Highly Hydrogen Permselective ZIF-8 Membranes Supported on Polydopamine Functionalized Macroporous Stainless-Steel-Nets

Aisheng Huang *[a], Qian Liu [a], Nanyi Wang [b], and Jürgen Caro [b]

Received (in XXX, XXX) Xth XXXXXXXXX 20XX, Accepted Xth XXXXXXXXX 20XX

DOI: 10.1039/b000000x

Inspired by the bio-adhesive ability of the marine mussel, highly hydrogen permselective ZIF-8 membranes are prepared on polydopamine-functionalized stainless-steel-nets (SSN). With polydopamine functionalization of SSN under a mild condition, the nucleation and growth of well-intergrown of ZIF-8 membranes are promoted through the formation of strong non-covalent and covalent bonds, which is helpful to enhance the membranes separation selectivity while maintaining high permeance. For binary mixtures at 100 ºC and 1 bar, the mixture separation factors of H_2/CO_2, H_2/N_2, H_2/CH_4 and H_2/C_3H_8, were found to be 8.1, 15.0, 23.2 and 329.7, which by far exceed the corresponding Knudsen coefficients and those of the as-reported ZIF-8 membranes. The ZIF-8 membranes also displayed high permeances with H_2 permeance higher than 2.1×10^{-5} $mol \cdot m^{-2} \cdot s^{-1} \cdot Pa^{-1}$ due to the high void volume of SSN.

Introduction

Metal-organic frameworks (MOFs) have attracted intense interest for gas adsorption and storage, molecular separation, and catalysis due to its highly diversified structures and pore sizes as well as specific adsorption affinities. [1-5] In the recent five years, a great deal of research effort has been focused on the preparation of supported MOF layers for their potential applications as separators, reactors, sensors. [6-12] In particular, zeolitic imidazolate frameworks (ZIFs), which consist of transition metals (Zn, Co) and imidazolates linkers, [13] have emerged as a novel porous material for the fabrication of molecular sieve membranes due to their zeolite-like properties such as permanent porosity, uniform pore size, exceptionally thermal and chemical stability. [12-31] So far, ZIF-7, [14] ZIF-8, [15-25] ZIF-22, [26] ZIF-69 [27] ZIF-71 [28] ZIF-90 [29-31] and ZIF-95 [32] membranes have sucessfully been prepared on various ceramic supports for single gas permeation or mixture gas separation.

Among the reported ZIF membranes, SOD ZIF-8 membranes, with highly thermal and chemical stability as well as small pore apertures (~ 0.34 nm), [13] are widely studied and of special interest for the fabrication of molecular sieve membranes. In the last three years, more and more effort has paid on the preparation of ZIF-8 membranes by in-situ growth, secondary growth, also liquid phase epitaxy method. [16-25, 33] However, it is often found that separate ZIF-8 crystals or islands rather than continuous layers were formed on the native ceramic supports by a direct solvothermal synthesis route because heterogeneous nucleation of ZIF-8 crystals on support surface is very poor. [17, 26] Therefore, seeds coating [20, 21] or chemical modification [17, 26] of the supports are applied to promote heterogeneous nucleation of ZIF-8 crystals on supports surface. Recently, inspired by the bio-adhesive ability of the marine mussel, we developed a simple, versatile and powerful synthesis strategy to prepare highly reproducible and selective ZIF-8 membranes without-seeding by using polydopamine (PDA) as a novel covalent linker. [34]

It should be noted that, in previous reports, the ZIF-8 membranes were usually prepared on porous oxide ceramics such as TiO_2 or Al_2O_3 disks. These ZIF-8 membranes have shown promising separation selectivity, but the hydrogen permeances are relatively low for practical applications due to the large flow resistance of gas transport through the thick ceramic supports (usual thickness 1 to 2 mm). In order to increase the permeance, Yao et al. prepared a highly permeable ZIF-8 membrane on a flexible nylon substrate with a contra-diffusion synthesis method. [22] However, the H_2/N_2 ideal selectivity of the ZIF-8 membrane is 3.7, indicating that there are unnegligible defects. Therefore, the challenge is to prepare ZIF-8 membranes with high permeance, while maintaining their high separation selectivity.

In the present work, we report a highly hydrogen permselective ZIF-8 membrane supported on a macroporous stainless-steel net (SSN). The thread woven for the SSN is about 25 µm thick, and the aperture of the SSN is about 30 × 30 µm in diameter. Therefore, the SSN has the same thickness as the thread diameter, which is much thinner - and thus has higher void volume - than a conventional α-Al_2O_3 support. As reported previously, [35] zeolite LTA membranes supported on SSN could show higher permeances. Therefore, it can be expected that the ZIF-8 membranes supported on SSN will show much higher permeances. However, to the best of our knowledge, there is no report on the preparation of ZIF-8 membranes on SSN.

Since there are less surface hydroxy groups on the SSN surfac to form covalent bonds with ZIF-8 framworks, the heterogeneous nucleation of ZIF-8 on SSN surfaces is very poor. In order to promote the nucleation and growth of well intergrown ZIF-8 layers on SSN, the SSN was functionalized by PDA before synthesis (Figure 1). Attributing to its adhesive ability through the formation of strong non-covalent and covalent bonds, [36, 37] the PDA is expected to promote the the nucleation and growth of well-intergrown of ZIF-8 membranes.

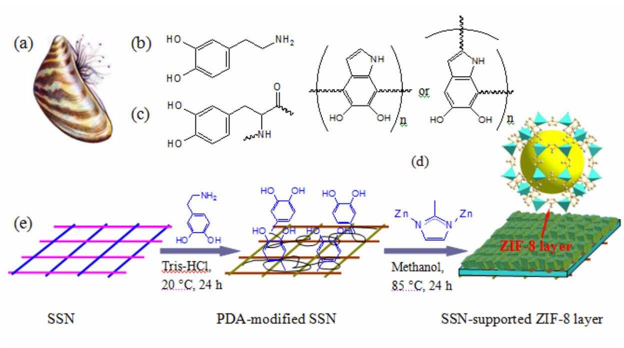

Fig. 1. Mussel with byssus threads (a), chemical structure of DPA (b), DOPA (c), and PDA (d), schema of the preparation of ZIF-8 molecular sieve membrane on PDA-functionalized SSN (e).

Experimental

Materials

Chemicals were used as received: zinc chloride (>99%, Merck), 2-methylimidazole (>99%, Aladin), sodium formate (>99%, Aladin), dopamine (DPA, 98%, Aladin), tris(hydroxymethyl) aminomethane (Tris-HCl, 99%, Aladin), methanol (99.9%, Aladin). Stainless-steel net (SSN, 500 mesh, 316L, Yingkaimo stainless-steel-net Co., Hebei, China) was cut as wafers of 18 mm in diameter and clean with ethanol under ultrasonic for 30 min before it was used as support.

Dopamine functionalization on the SSN surface

The Dopamine (2 mg/mL) was dissolved in 10 mM Tris-HCl (pH 8.5) in an open watch glass (150 mm in diameter). And then SSN wafers and α-Al_2O_3 disks were treated with dopamine at 25 °C for 24 h, leading to polydopamine layer being deposited on the supports surface. [34]

Synthesis of ZIF-8 membrane on PDA-modified SSN surface

The ZIF-8 membrane was prepared according to the following procedure as reported elsewhere with minor modification. [16] A solid mixture of 0.538 g zinc chloride, 0.648 g 2-methylimidazole and 0.268 g sodium formate was dissolved in 50 ml methanol by ultrasonic treatment. PDA-treated or PDA-free supports were placed horizontally in a Teflon-lined stainless steel autoclave which was filled with synthesis solution, and heated at 85 °C in air oven for 24 h.

Characterization of ZIF-8 membranes

The ZIF-8 membrane morphology was investigated by field emission scanning electron microscopy (FESEM). FESEM micrographs were taken on an S-4800 (Hitachi) with a cold field emission gun operating at 4 kV and 10 μA. The phase purity and crystallinity of the ZIF-8 membranes were confirmed by X-ray diffraction (XRD). The XRD patterns were recorded at room temperature under ambient conditions with Bruker D8 ADVANCE X-ray diffractometer with CuKa radiation at 40 kV and 40 mA.

Single gas permeation and mixed gases separation

For the single gas permeation and mixed gases separation, the supported ZIF-8 membrane was sealed in a permeation module with silicone O-rings. The feed gases were fed to the top-side of the membrane, and sweep gas was fed on the permeate side to keep the concentration of permeating gas low providing a driving force for permeation. The total pressure on each side of the membrane was atmospheric. For both single and mixture gas permeation, the fluxes of feed and sweep gases were determined with mass flow controllers, and a calibrated gas chromotograph (Echrom A90) was used to measure the gas concentrations, as shown elsewhere. [26] The separation factor $\alpha_{i,j}$ of a binary mixture permeation is defined as the quotient of the molar ratios of the components (i, j) in the permeate, divided by the quotient of the molar ratio of the components (i, j) in the retentate, as shown in following.

$$\alpha_{i/j} = \frac{y_{i,Perm} / y_{j,Perm}}{y_{i,\mathrm{Ret}} / y_{j,\mathrm{Ret}}}$$

Results and discussion

By simple immersion of the SSN supports in buffered aqueous solution of DPA (pH=8.5) at room temperature for 24 h, DPA polymerizes to PDA and readily deposits on the SSN support (Fig. S1b). Then the ZIF-8 membranes were prepared on the PDA-functionalized SSN at 85 °C for 24 h. In good agreement with our previous report, [34] it is difficult to direct heterogeneous nucleation and growth of a continuous ZIF-8 layer on the non-modified SSN surface (Figs. 2a, b), and tremendous pinholes are easily observed since there are no additional linkage groups in ZIF-8 frameworks to form covalent bonds with the surface OH groups of the SSN supports.

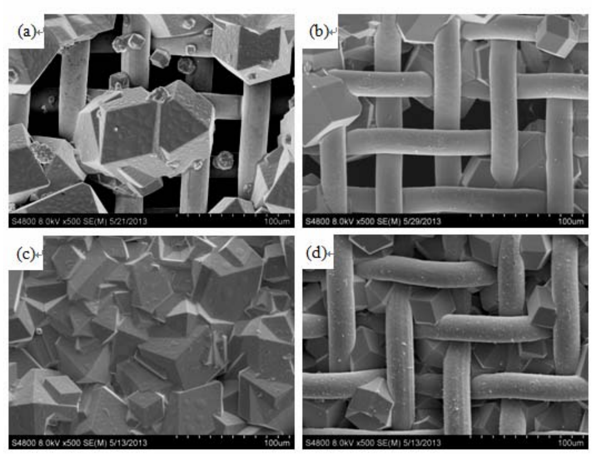

Fig. 2. FESEM images of upper side (a) and down side (b) of the ZIF-8 layer prepared for 24 h on non-modified SSN, FESEM images of upper side (c) and down side (d) of the of ZIF-8 membrane prepared for 24 h on PDA-functionalized SSN. The attributes “upper” and “down” refer to the horizontal orientation of the SSN in ZIF-8 membrane synthesis.

On the contrary, after modification of SSN with PDA before solvothermal reaction, a dense ZIF-8 layer could be easily formed on the PDA-functionalized SSN. As shown in Fig. 2c, the upper side of the horizontally oriented SSN surface is completely covered with well intergrown rhombic dodecahedron crystals, and no visible cracks, pinholes or other defects are observed. In the present work, both amino-groups and hydroxyl amino-groups of PDA can coordinate to the free Zn^{2+} centers and bind the growing nano-crystals directly. Therefore, covalent bonds (Zn-N and Zn-O) between the growing ZIF-8 layer and the support is formed to anchor the ZIF-8 crystals for membrane formation. [26] The formation of a dense ZIF-8 layer is also confirmed by the down side image of the ZIF-8 membrane. It can be seen that the ZIF-8 crystals with comparable size of about 40 µm are grown in the meshes of the SSN and close it completely (Fig. 2d). Interestingly, the SSN acts as framework for the formation of a dense ZIF-8 membrane, just like the steel bars used to reinforce concrete in building construction. Such a “reinforced concrete” structure can increase the mechanical stability of the ZIF-8 membrane layer sticking to the support surface. Indeed, as shown in Fig. S2, the membrane morphology keeps unchanged after 10 min ultrasonic treatment in ethanol, and no crystals exfoliation or detachment from the membrane layer can be found.

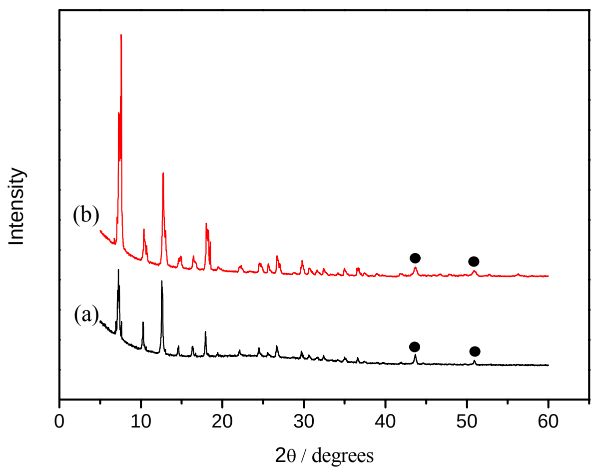

Fig. 3. XRD patterns of the ZIF-8 layer prepared on non-modified SSN (a), and PDA-functionalized SSN. (●): SSN, (not marked): ZIF-8 crystals.

Fig. 3 shows the XRD patterns of the ZIF-8 layer prepared on non-modified and PDA-functionalized SSN. It can be seen that all peaks of the membrane layer match well with the reported structural data of ZIF-8 besides SSN signals, [16, 34] indicating that a phase-pure ZIF-8 membrane with high crystallinity has been formed on the SSN supports. In comparison with the XRD pattern of the ZIF-8 membrane prepared on non-modified SSN, the XRD pattern of the ZIF-8 membrane prepared on PDA-functionalized SSN exhibits a stronger intensity due to the formation of a denser membrane layer. Fig. 4 shows the FESEM images of ZIF-8 membranes prepared on the PDA-functionalized SSN at 85 °C for different synthesis times. As shown in Fig. 4a, only amorphous phases rather than ZIF-8 crystals are observed on the SSN surface after 4 h. Up to a crystallization time of 8 h, ZIF-8 crystals with clear facets have been formed on SSN surface, but there are observable inter-crystalline gaps between the ZIF-8 crystals (Fig. 4b). With increasing crystallization time up to 24 h, the ZIF-8 crystals grow together and form a homogeneous and compact ZIF-8 membrane (Fig. 4d). It is worth to note that the PDA functionalization is done under mild conditions (simple immersion in buffered aqueous solution of DPA at room temperature) in comparison with the previously proposed chemical modification methods, [26, 29] which is helpful to prepare ZIF-8 membranes at large-scale and reduce the costs of the membrane manufacturing. Further, it is found that PDA functionalization also facilitates the formation of dense zeolite LTA membranes on PDA-functionalized SSN (Fig. S3).

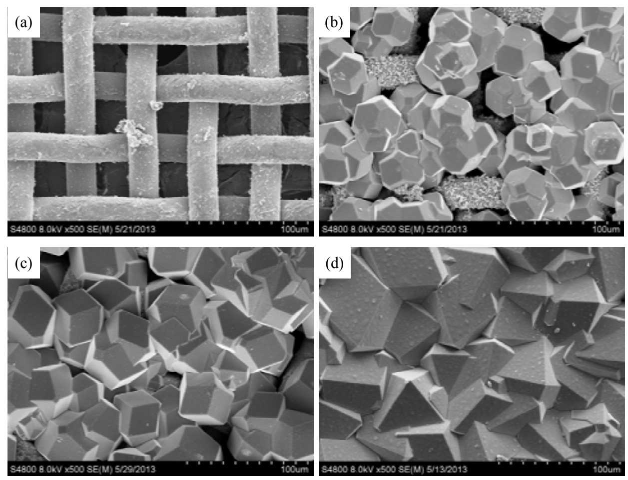

Fig. 4. FESEM images of ZIF-8 layer prepared on DPA-functionalized SSN with different synthesis time: 4 h (a), 8 h (b), 16 h (c), and 24 h (d).

The volumetric flow rates of the single gases H_2, CO_2, N_2, CH_4 and C_3H_8 as well as the eqimolar binary mixtures of H_2 with CO_2, N_2, CH_4 and C_3H_8 were measured by using the Wicke-Kallenbach technique. [26, 29] The permeances and separation factors are summarized in Table S1. Fig. 5 shows the permeances of the single gases through the SSN-supported ZIF-8 membrane as a function of the kinetic diameters of the permeating molecules at 100 ºC and 1 bar. As shown in Fig. 5 and Table S1, the gas permeances clearly depend on the molecular size with the order: $H_2 > CO_2 > N_2 > CH_4 > C_3H_8$. The H_2 permeance of 2.66×10^{-5} $mol\cdot m^{-2}\cdot S^{-1}\cdot Pa^{-1}$ is much higher than that of the other gases due to the small kinetic diameter of hydrogen with 0.29 nm. The ideal separation factors of H_2 from CO_2, N_2, CH_4 and C_3H_8, determined as the ratio of the single component permeances, are 8.8, 15.4, 24.6 and 442.5 (Table S1), indicating that the ZIF-8 membrane displays high H_2 permselective.

The molecular sieve performance of the ZIF-8 membrane was confirmed by the separation of equimolar mixtures of H_2 and CO_2, N_2, CH_4, and C_3H_8 at 100 ºC and 1 bar. As shown in Table S1, comparing with the H_2 single gas permeance, only a slight reduction of H_2 permeance in mixtures is observed, with a H_2 permeance of about $2.12\sim2.46\times10^{-5}$ $mol\cdot m^{-2}\cdot S^{-1}\cdot Pa^{-1}$, suggesting that the larger molecules (CO_2, N_2, CH_4, and C_3H_8) only slightly hinder the permeation of the highly mobile H_2. For the equimolar mixtures, the mixture separation factors of H_2/CO_2, H_2/N_2, H_2/CH_4 and H_2/C_3H_8 are 8.1, 15.0, 23.2 and 329.7 (inset in Fig. 2), which by far exceed the corresponding Knudsen coefficients

(4.7, 3.7, 2.8 and 4.7, respectively). Attributing to the amazing adhesive ability of PDA, the PDA modification is helpful to synthesize well-intergrown, highly selective and reproducibile ZIF-8 membranes (Table S2). The average H_2/CH_4 selectivity is 22.5±0.55 (standard deviation) for three independent membranes.

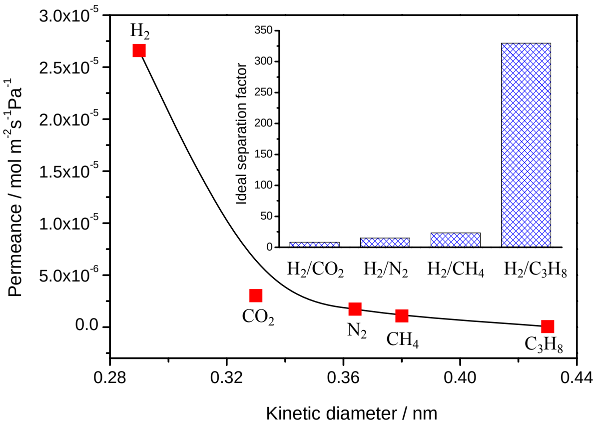

Fig. 5. Single gas permeances on the ZIF-8 membrane prepared on PDA-functionalized SSN at 100 ºC and 1 bar as a function of the kinetic diameter. The inset shows the mixture separation factors for H_2 over other gases from equimolar mixtures as determined by gas chromatography.

Table 1. Comparison of the gas separation performances of the ZIF-8 membranes prepared on difference supports.

Support	Thickness (μm) [a]	Separation performance		Ref.
		P (H_2) [b]	H_2/CH_4 selectivity	
1000 μm [c] TiO_2	30	0.6	12.6	14
2000 μm Al_2O_3	20	1.7	13.0	15
500 μm Al_2O_3 HF	6	9.9	3.9	17
150 μm YSZ HF	2	12.3	13.0	19
80 μm Nylon	16	126	3.7 [d]	20
1000 μm Al_2O_3	20	1.6	26.4	31
30 μm SSN	30	242	23.2	This work

[a] membranes thickness, [b] H_2 permeance ($\times 10^7$mol·m^{-2}·S^{-1}·Pa^{-1}), [c] supports thickness, [d] H_2/N_2 selectivity.

We have reported the first continuous ZIF-8 membrane on TiO_2 disks by microwave-assisted solvothermal synthesis method, with a good H_2/CH_4 selectivity of 12.6, but a relative low hydrogen permeance of 0.6 x 10^{-7} mol·m^{-2}·S^{-1}·Pa^{-1} due to the thick membrane layer (~30 μm). [16] By reducing the membrane thickness to 20 μm, Jeong et al. reported a higher permeance ZIF-8 membrane (1.7 x 10^{-7} mol·m^{-2}·s^{-1}·Pa^{-1}) prepared on Al_2O_3 disks with H_2/CH_4 selectivity of 13.0. [17] It should be noted not only the membrane thickness but also the supports materials and thickness have great effect on the permeance (Table 1). Lai and colleagues prepared high permselective ZIF-8 membranes on YSZ hollow fibers (HF) through secondary growth with seeding. [21] Wang and colleagues synthesized a highly permeable ZIF-8 membrane on a flexible nylon polymer with a contra-diffusion synthesis method. [22] However, the H_2/N_2 selectivity of the ZIF-8 membrane was only 3.7, indicating macroporous defects were presented in membrane layer. In the present work, attributing to the formation of strong non-covalent and covalent bonds between the SSN and ZIF-8 membrane layer, [36] the ZIF-8 nutrients are attracted and anchored onto the support surface for the facile synthesis of well-intergrown ZIF-8 membranes, which is helpful to reduce the defect density and thus enhancing the separation selectivity. Further, compared with literature data of H_2 permeances on ZIF-8 membranes (Table 1) and other MOF/zeolite membranes (Table S3), the ZIF-8 membrane developed in this study shows a much higher H_2 permeance. The obtained high H_2 permeance of the ZIF-8 membrane is attributed to the highly void volume of SSN, which is helpful to reduce the flow resistance of gas transport. In addition, the ZIF-8 membrane prepared on PDA-functionalized SSN also shown high thermal stability (Fig. 6), and can keep its high H_2 permselectivity when the H_2 partial pressure increases from 0.5 to 1.5 bars (Fig. S4).

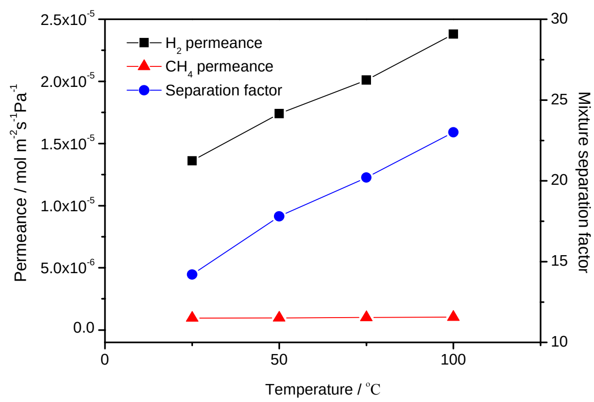

Fig. 6. Gas permeances and H_2/CH_4 selectivity of the ZIF-8 membrane supported on PDA-functionalized SSN as a function of the temperature at 1 bar.

Conclusions

In conclusion, we report a facile and universal seeding-free method of growing dense ZIF-8 membranes on thin and macroporous stainless-steel nets to enhance the permeance by using an attachment chemistry based on polydopamine, a polymer inspired by marine mussels for adhesion to surfaces. Attributing to the amazing adhesive ability of PDA, the ZIF-8 nutrients are attracted and anchored onto the support surface for the formation of well-intergrown and highly selective ZIF-8 membranes. For binary mixtures at 100 ºC and 1 bar, the mixture separation factors of H_2/CO_2, H_2/N_2, H_2/CH_4 and H_2/C_3H_8, were found to be 8.1, 15.0, 23.2 and 329.7, respectively, which by far exceed the corresponding Knudsen coefficients. The ZIF-8 membranes also displayed high permeance with H_2 permeance higher than 2.1 x 10^{-5} mol·m^{-2}·s^{-1}·Pa^{-1}, which by far exceed those of the as-reported ZIF-8 membranes, due to the high void volume of SSN. Further, the PDA functionalization also supports the formation of zeolite LTA growing on the inexpensive stainless-steel nets.

Acknowledgements

Financially supported by the National Natural Science Foundation of China (Grant No. 21276262), Chinese Academy of Science Visiting Professorship for Senior International Scientists

(Grant No. 2013T1G0047), and the Starting Research Fund of Team Talent from NIMTE (Grant No. Y20808A05) are acknowledged. The authors thank Mr. H. Chen for help in measurement of FESEM.

References

[a] *Institute of New Energy Technology, Ningbo Institute of Material Technology and Engineering, CAS, 519 Zhuangshi Road, 315201 Ningbo, P. R. China. E-mail: huangaisheng@nimte.ac.cn*
[b] *Institute of Physical Chemistry and Electrochemistry Leibniz University Hannover, Callinstraße 3-3A, D-30167 Hannover, Germany*

† Electronic Supplementary Information (ESI) available: Experimental details, photographs, SEM and XRD of the ZIF-8 membrane, separation performances. See DOI: 10.1039/b000000x/

1 H. Li, M. Eddaoudi, M. O'Keeffe and O. M. Yaghi, *Nature,* 1999, **402**, 276.
2 J. S. Seo, D. Whang, H. Lee, S. I. Jun, J. Oh, Y. J. Jeon and K. Kim, *Nature,* 2000, **404**, 982.
3 L. J. Murray, M. Dincâ and J. R. Long, *Chem. Soc. Rev.,* 2009, **38**, 1294.
4 O. M. Yaghi, M. O'Keeffe, N. W. Ockwig, H. K. Chae, M. Eddaoudi and J. Kim, *Nature* 2003, **423**, 705.
5 J. R. Li, R. J. Kuppler and H. C. Zhou, *Chem. Soc. Rev.,* 2009, **38**, 1477.
6 S. Hermes, F. Schröder, R. Chelmowski, C. Wöll and R. A. Fischer, *J. Am. Chem. Soc.,* 2005, **127**, 13744.
7 E. Biemmi, C. Scherb and T. Bein, *J. Am. Chem. Soc.,* 2007, **129**, 8054.
8 R. Ranjan and M. Tsapatsis, *Chem. Mater.,* 2009, **21**, 4920.
9 G. Lu, O. K. Farha, W. Zhang, F. Huo and J. T. Hupp, *Adv. Mater.*, 2012, **24**, 3970.
10 Y. Yoo, Z. Lai and H. -K. Jeong, *Microporous Mesoporous Mater.,* 2009, **123**, 100.
11 Y. Yoo, V. Varela-Guerrero and H.-K. Jeong, *Langmuir,* 2011, **27**, 2652.
12 S. Aguado, C. H. Nicolas, V. Moizan-Baslé, C. Nieto, H. Amrouche, N. Bats, N. Audebrandd and D. Farrusseng, *New J. Chem.,* 2011, **35**, 41.
13 K. S. Park, Z. Ni, A. P. Côté, J. Y. Choi, R. Huang, F. J. Uribe-Romo, H. K. Chae, M. O'Keeffe and O. M. Yaghi, *Proc. Natl. Acad. Sci. U. S. A.,* 2006, **103**, 10186.
14 Y. Li, F. Liang, H. Bux, A. Feldhoff, W. Yang and J. Caro, *Angew. Chem. Int. Ed.,* 2010, **49**, 548.
15 S. R. Venna and M. A. Carreon, *J. Am. Chem. Soc.,* 2010, **132**, 76.
16 H. Bux, F. Liang, Y. Li, J. Cravillon, M. Wiebcke and J. Caro, *J. Am. Chem. Soc.,* 2009, **131**, 16000.
17 M. C. McCarthy, V. Varela-Guerrero, G. V. Barnett and H. -K. Jeong, *Langmuir,* 2010, **26**, 14636.
18 H. T. Kwon and H.-K. Jeong, *J. Am. Chem. Soc.,* 2013, **135**, 10763.
19 G. Xu, J. Yao, K. Wang, L. He, P. A. Webley, C. Chen and H. Wang, *J. Membr. Sci.,* 2011, **385–386**, 187.
20 Y. Pan and Z. Lai, *Chem. Commun.,* 2011, **47**, 10275.
21 Y. Pan, B. Wang and Z. Lai, *J. Membr. Sci.,* 2012, **421–422**, 292.
22 J. Yao, D. Dong, D. Li, L. He, G. Xu and H. Wang, *Chem. Commun.*, 2011, **47**, 2559.
23 E. Barankova, N. Pradeep and K.-V. Peinemann, *Chem. Commun.,* 2013, **49**, 9419.
24 K. Huang, Z. Dong, Q. Li and W. Jin, *Chem. Commun.*, 2013, **49**, 10326.
25 Z. Xie, J. Yang, J. Wang, J. Bai, H.Yin, B. Yuan, Ji. Lu, Y. Zhang, L. Zhou and C. Duan, *Chem. Commun.*, 2012, **48**, 5977.
26 A. Huang, H. Bux, F. Steinbach and J. Caro, *Angew. Chem. Int. Ed.,* 2010, **49**, 4958.
27 Y. Liu, E. Hu, E. A. Khan and Z. Lai, *J. Membr. Sci.,* 2010, **353**, 36.
28 X. Dong and Y. S. Li, *Chem. Commun*., 2013, **49**, 1196.
29 A. Huang, W. Dou and J. Caro, *J. Am. Chem. Soc.,* 2010, **132**, 15562.
30 A. Huang, N. Wang, K. Kong and J. Caro, *Angew. Chem. Int. Ed.* 2012, **51**, 10551.
31 A. J. Brown, J. R. Johnson, M. E. Lydon, W. J. Koros, C. W. Jones and S. Nair, *Angew. Chem. Int. Ed.,* 2012, **51**, 10615.
32 A. Huang, Y. Chen, N. Wang, Z. Hu, J. Jiang and J. Caro, *Chem. Commun.,* 2012, **48**, 10981.
33 O. Shekhaha and M. Eddaoudi, *Chem. Commun.*, 2013, **49**, 10079.
34 Q. Liu, N. Wang, J. Caro and A. Huang, *J. Am. Chem. Soc.,* 2013, **135**, 17679.
35 X. Yin, G. Zhu, W. Yang, Y. Li, G. Zhu, R. Xu, J. Sun, S. Qiu and R. Xu, *Adv. Mater.,* 2005, 17, 2006.
36 J. H. Waite, and M. L. Tanzer, *Science* 1981, **212**, 1038.
37 H. Lee, S. M. Dellatore, W. M. Miller, and P. B. Messersmith, *Science* 2007, **318**, 426